Visual Neuroscience (1999), **16**, 1115–1121. Printed in the USA.
Copyright © 1999 Cambridge University Press 0952-5238/99 $12.50

Linear and nonlinear contributions to orientation tuning of simple cells in the cat's striate cortex

JUSTIN L. GARDNER, AKIYUKI ANZAI, IZUMI OHZAWA, AND RALPH D. FREEMAN

Groups in Bioengineering and Vision Science, School of Optometry, University of California, Berkeley

(RECEIVED March 4, 1999; ACCEPTED June 30, 1999)

Abstract

Orientation selectivity is one of the most conspicuous receptive-field (RF) properties that distinguishes neurons in the striate cortex from those in the lateral geniculate nucleus (LGN). It has been suggested that orientation selectivity arises from an elongated array of feedforward LGN inputs (Hubel & Wiesel, 1962). Others have argued that cortical mechanisms underlie orientation selectivity (e.g. Sillito, 1975; Somers et al., 1995). However, isolation of each mechanism is experimentally difficult and no single study has analyzed both processes simultaneously to address their relative roles. An alternative approach, which we have employed in this study, is to examine the relative contributions of linear and nonlinear mechanisms in sharpening orientation tuning. Since the input stage of simple cells is remarkably linear, the nonlinear contribution can be attributed solely to cortical factors. Therefore, if the nonlinear component is substantial compared to the linear contribution, it can be concluded that cortical factors play a prominent role in sharpening orientation tuning. To obtain the linear contribution, we first measure RF profiles of simple cells in the cat's striate cortex using a binary m-sequence noise stimulus. Then, based on linear spatial summation of the RF profile, we obtain a predicted orientation-tuning curve, which represents the linear contribution. The nonlinear contribution is estimated as the difference between the predicted tuning curve and that measured with drifting sinusoidal gratings. We find that measured tuning curves are generally more sharply tuned for orientation than predicted curves, which indicates that the linear mechanism is not enough to account for the sharpness of orientation-tuning. Therefore, cortical factors must play an important role in sharpening orientation tuning of simple cells. We also examine the relationship of RF shape (subregion aspect ratio) and size (subregion length and width) to orientation-tuning halfwidth. As expected, predicted tuning halfwidths are found to depend strongly on both subregion length and subregion aspect ratio. However, we find that measured tuning halfwidths show only a weak correlation with subregion aspect ratio, and no significant correlation with RF length and width. These results suggest that cortical mechanisms not only serve to sharpen orientation tuning, but also serve to make orientation tuning less dependent on the size and shape of the RF. This ensures that orientation is represented equally well regardless of RF size and shape.

Keywords: Linear summation, Receptive field, Orientation selectivity, Expansive nonlinearity

Introduction

Receptive-field (RF) characteristics change dramatically between the cat's lateral geniculate nucleus (LGN) and visual cortex. Neurons in the LGN exhibit concentric center-surround RFs and respond to any stimulus orientation (Hubel & Wiesel, 1961). On the other hand, simple cells in the striate cortex have RFs that consist of elongated discrete regions of adjacent ON and OFF areas, and are selective to stimulus orientation (Hubel & Wiesel, 1959, 1962). The classical explanation of this change is a feedforward system in which LGN cell RFs of identical polarity are aligned along a single axis. This comprises the elongated simple cell RF and provides the synaptic inputs that form the basis for the observed orientation selectivity (Hubel & Wiesel, 1962).

Understanding the neural mechanisms responsible for the orientation tuning is of fundamental importance, and a number of studies have been designed to test the feedforward hypothesis. For example, extracellular recordings of LGN afferents after pharmacological blockage of cortical cell activity (Chapman et al., 1991) and a cross-correlation analysis of LGN and simple-cell spikes (Reid & Alonso, 1995) have lent support to the suggestion that LGN cell RFs are aligned along the axis of cells' preferred orientation. Inactivating the cortical network by cooling does not effectively disrupt the orientation selectivity of synaptic potentials (Ferster et al., 1996), which is consistent with a feedforward excitatory model of orientation selectivity.

However, other studies suggest a prominent role for intracortical mechanisms. For example, orientation selectivity is greatly

Address correspondence and reprint requests to: Ralph D. Freeman, University of California, School of Optometry, 360 Minor Hall #2020, Berkeley, CA 94720-2020, USA. E-mail: freeman@pinoko.berkeley.edu

reduced following iontophoretic application of the GABA antagonist bicuculline (Sillito, 1975; Tsumoto et al., 1979; Sillito et al., 1980), and it has been suggested that cortical inhibition acts to determine orientation selectivity by inhibiting responses to nonoptimal orientations (Sillito, 1975; Hata et al., 1988). However, the inhibition was later found to be strongest at the optimal orientation (Ferster, 1986; DeAngelis et al., 1992; Douglas et al., 1991). Furthermore, intracellular blockage of GABA-A mediated inhibition does not disrupt orientation selectivity (Nelson et al., 1994). It is also possible to account for orientation selectivity by recurrent cortical circuitry (Douglas et al., 1995; Somers et al., 1995). Somers et al. (1995) have proposed a model in which a dominant source of orientation-selective input comes from recurrent excitation whereas excitatory feedforward LGN inputs are only weakly tuned for orientation. The model also incorporates cortical inhibition which acts nonspecifically to orientation and serves to sharpen the orientation tuning by raising the spiking threshold and creating an iceberg effect.

Although these results are instructive, none of them has examined both feedforward and cortical mechanisms to address the relative contributions of each. This is because isolation of each mechanism is experimentally difficult. An alternative approach, which is employed in our study, is to examine the relative contributions of *linear* and *nonlinear* mechanisms in sharpening orientation tuning. This approach allows us to conclude that cortical mechanisms play an important role in sharpening orientation tuning if the contribution of nonlinear mechanisms is significant relative to that of linear mechanisms.

The basis of this inference is as follows. A common simple-cell model consists of a linear filter followed by a static nonlinearity (e.g. Movshon et al., 1978; Tolhurst & Dean, 1987; Albrecht & Geisler, 1991; Heeger, 1992*b*; DeAngelis et al., 1993; Anzai et al., 1999*b*), and the static nonlinearity has been identified as an expansive function (e.g. Emerson et al., 1989; Anzai et al., 1999*b*). The linear filter represents the effect of both feedforward LGN inputs (e.g. Reid & Alonso, 1995; Jagadeesh et al., 1997) and cortical mechanisms such as spatially opponent inhibition (Ferster, 1988; see also Pollen & Ronner, 1982; Troyer et al., 1998). On the other hand, the expansive nonlinearity of simple cells is assumed to be solely the consequence of cortical factors such as cellular properties involved in the spike-triggering mechanism as well as nonlinear inputs from the cortical network. Note that the effects of subcortical nonlinearities do not appear to be manifested by cortical neurons since the input stage of simple cells is remarkably linear (e.g. Jagadeesh et al., 1997). Therefore, if nonlinear mechanisms make a significant contribution to the sharpness of orientation tuning compared to linear mechanisms, then it can be concluded that cortical factors must play an important role in sharpening orientation tuning.

We report here an examination of linear and nonlinear mechanisms in orientation tuning. To obtain the linear contribution, we first measure RF profiles using a binary m-sequence noise stimulus. Then, we obtain a predicted orientation-tuning curve based on linear spatial summation of the RF profile. The predicted tuning curve thus represents the linear contribution. We also measure a detailed orientation-tuning curve using drifting sinusoidal gratings. The difference between the predicted and measured tuning curves provides an estimate of the nonlinear contribution. We quantify this nonlinear contribution as an exponent of the expansive nonlinearity, and compare that with the linear contribution. Our results indicate that linear mechanisms are not sufficient to account for the sharpness of orientation tuning of most simple cells, suggesting a significant contribution of nonlinear mechanisms. Therefore, cortical mechanisms play a prominent role in sharpening orientation tuning of simple cells.

Methods

Recording and physiology

Details of the surgical and physiological procedures are as described elsewhere (Anzai et al., 1999*a*,*b*) Briefly, extracellular recordings were made from simple cells in the striate cortex of anesthetized and paralyzed adult cats. Recordings from well isolated single units were made with the use of two tungsten-in-glass electrodes (Levick, 1972). After a single unit was identified by the waveform of its response, the RF extents, optimal orientation, and spatial frequency were measured qualitatively using sinusoidal gratings. Then, an orientation-tuning curve was measured as the first harmonic responses to sinusoidal gratings in which the position, size, and spatial frequency were set to the optimal for the cell and the orientation was varied randomly to have one of seven or more values spaced in 10–15-deg steps around the optimal value. The gratings were drifted at a temporal frequency of 2 Hz, and two possible directions of grating motion were tested for each orientation (i.e. directions orthogonal to the orientation).

Two-dimensional (2D) spatio-temporal RFs were mapped with white noise stimuli generated according to binary m-sequences (Sutter, 1992). A roughly circular-shaped stimulus patch large enough to cover the RF of the cell was used. The patch was divided into 128 equally sized squares. The luminance of each square was modulated every 40 ms to be either 18 cd/m^2 above or below the mean luminance (20 cd/m^2) of the cathode ray tube display. An RF map is obtained by cross-correlation of the stimulus sequence and the resulting spike train of the cell. The RF represents a spatio-temporal structure that characterizes a linear approximation to the transformation between the stimulus and response, and is a function of the position of the stimulus in visual space and time (the cross-correlation delay). Cells are classified as simple based on RF organization (Hubel & Wiesel, 1959) and the degree of first harmonic modulation in their response to drifting sinusoidal gratings (Skottun et al., 1991).

Data analysis

To obtain parameters of the orientation-tuning curve, we fit a Gaussian to the tuning data using the Levenberg–Marquardt algorithm (Press et al., 1988). The equation for the Gaussian is

$$r(\theta) = Ae^{-(\theta-\theta_{opt})^2/2\sigma_\theta^2} + A_{off}, \quad (1)$$

where $r(\theta)$ is the response amplitude at orientation θ. Parameters A and A_{off} are the peak response amplitude and the amplitude offset (usually near zero), respectively. θ_{opt} denotes the optimal orientation (the center of the Gaussian), and σ_θ is the standard deviation of the Gaussian. Halfwidth of the orientation-tuning curves is defined as half the width of the Gaussian at half the peak height above the amplitude offset.

To obtain a predicted orientation-tuning curve from the spatio-temporal RF measured by the white noise stimuli, we transformed the RF into the frequency domain by applying Fourier analysis. For each cell, the spatial profile of the RF (Fig. 1a) at the optimal correlation delay (defined as the delay which produces the largest

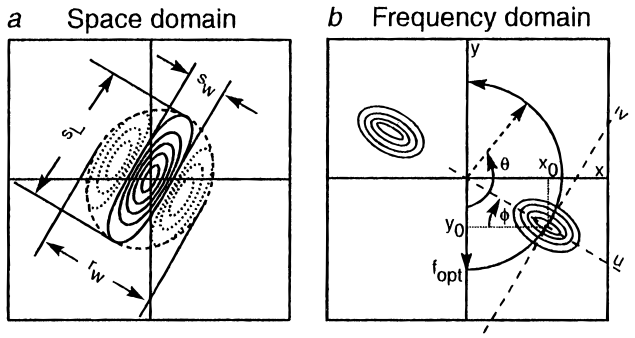

Fig. 1. (a) Space-domain representation of the RF of a simple cell. Solid contours represent a bright-excitatory subregion and dotted lines represent dark-excitatory subregions. The dashed line represents the extent of the RF. s_L and s_w refer to the length and width of a subregion, respectively. r_w denotes the width of the RF. Subregion aspect ratio (s_L/s_w) is estimated for each cell using RF parameters obtained in the frequency domain (see text for a definition). (b) Frequency-domain representation of the RF of a simple cell. See text for details of obtaining predicted orientation-tuning curves.

sum of squared responses and has a population average of 52 ± 8.7 S.D. ms) is chosen and the 2D discrete Fourier transform taken. This yields a 2D amplitude spectrum (Fig. 1b), which is symmetric about the origin. Then, we fit one-half of the spectrum with a 2D Gaussian:

$$R(u,v) = Ae^{-[(u^2/2\sigma_u^2)+(v^2/2\sigma_v^2)]} + A_{off}, \tag{2}$$

where

$$u = (x - x_0)\cos(\phi) + (y - y_0)\sin(\phi),$$

$$v = -(x - x_0)\sin(\phi) + (y - y_0)\cos(\phi).$$

A and A_{off} denote the amplitude and the amplitude offset, respectively. σ_u and σ_v are the standard deviations of the Gaussian along the u and v axes (dashed lines in Fig. 1b), respectively. The u–v coordinate is obtained by shifting the x–y coordinate of the spectrum by (x_0, y_0) and then rotating it around the origin through the angle ϕ, where (x_0, y_0) is the center coordinate of the Gaussian and ϕ is the rotation angle of the Gaussian.

A predicted orientation-tuning curve is obtained by sweeping out a semicircle centered on the origin of the x–y coordinate with radius (f_{opt}) equal to the spatial frequency of the sinusoidal gratings which were used to measure the orientation-tuning curves (see Fig. 1b). The value of each point on the semicircle represents a predicted response amplitude of the cell to a sinusoidal grating of an orientation θ equal to the angle of the point. The predicted tuning curve is then fit with a Gaussian [eqn. (1)] to obtain parameters of the Gaussian and estimate the halfwidth of the tuning curve.

In addition, we estimated the aspect ratio of the RF subregion and the number of subregions to examine their effects on the sharpness of the orientation tuning. Aspect ratio of the RF subregion is defined in the space domain (Fig. 1a) as the extent of the RF subregion along the direction of the RF orientation (s_L) divided by the extent along the orthogonal direction (s_w), that is,

$$\text{Subregion Aspect Ratio} = s_L/s_W. \tag{3}$$

We estimated the subregion length s_L as

$$s_L = 2\sqrt{2}\sigma_L, \tag{4}$$

where

$$\sigma_L = 1/(\pi\sigma_v).$$

The subregion length (s_L) corresponds to the length of the RF envelope in the space domain at 37% ($1/e$) of its maximum amplitude. The subregion width s_W is obtained as

$$s_W = 1/(2f_o), \tag{5}$$

where f_o is the optimal spatial frequency of the cell, which is defined by the distance between the center of the 2D Gaussian (x_0, y_0) and the origin of the x–y coordinate system in Fig. 1b.*

The number of subregions in the RF is estimated as

$$\text{Number of subregions} = 2\sqrt{2}\sigma_W/s_W \tag{6}$$

where

$$\sigma_w = 1/(\pi\sigma_u).$$

The term $2\sqrt{2}\sigma_W$ corresponds to the width of the RF envelope in the space domain (r_w in Fig. 1a) at 37% ($1/e$) of its maximum amplitude.

Results

We have recorded from a total of 146 simple cells from 28 adult cats. We restricted the analysis to 37 cells whose orientation-tuning curves had been measured at close to the optimal spatial frequency with a sufficient number of different orientations to constrain the Gaussian fit. For the chosen cells, Gaussian curves provided excellent fits to the data points and the best-fitting parameters had variance within 10% of the parameter values. Most cells responded better to gratings drifting in one direction (preferred direction) than to those drifting in the opposite direction (nonpreferred direction). However, as reported previously (Campbell et al., 1968), the halfwidth of the orientation-tuning curve measured for the preferred direction was similar to and did not differ in any consistent way from the halfwidth for the nonpreferred direction. We therefore analyzed orientation-tuning curves for only one direction: either the preferred direction (33 cells including three nondirectional cells) or the nonpreferred direction (four cells) when the tuning curve for the preferred direction was not constrained well for the Gaussian fit.

As expected from previous studies (Jones & Palmer, 1987*b*), we find that the peak orientation of the cell from both measured and predicted tuning curves are well matched (linear regression analysis: $r^2 = 0.957$, slope = 0.986, $P < 0.01$) but that the half-

*Because s_W and s_L are estimated differently [eqns. (4) and (5)], our subregion aspect ratio may be underestimated by a small constant factor. However, this will not affect our results since this constant factor will serve only to shift all of the points in the log–log graph of Fig. 4a to the right by the same amount.

widths of these curves are not (cf. Volgushev et al., 1996). Fig. 2a shows a scatter plot of measured *versus* predicted halfwidths of the orientation-tuning curves for the population of cells examined. Most of the data points fall below the diagonal line, indicating that the measured tuning halfwidth is smaller than predicted. Histograms of predicted (Fig. 2b, dark bars) and measured (Fig. 2c, light bars) halfwidths are shown above and to the right of the scatter plot, respectively. The measured halfwidths range from 9.0 to 28.7 deg, which are similar to values reported in other studies (Campbell et al., 1968; Henry et al., 1974; Rose & Blakemore, 1974; Watkins & Berkley, 1974). The distribution has a mean of 15.8 deg. In contrast, the distribution for the predicted halfwidths ranges from 9.3 to 59.8 deg and has a mean of 28.3 deg. The difference between the means of the two distributions is statistically significant (*t*-test of unequal variances: $P < 0.01$). The distribution of the predicted halfwidths also has a larger standard deviation (10.0 deg) than that (5.7 deg) of the measured halfwidths (F-test: $P < 0.01$). These discrepancies between the measured and the predicted tuning curves can be accounted for by the expansive nonlinearity exhibited by simple cells.

As mentioned earlier, simple cells are modeled as a linear filter followed by an expansive nonlinearity (e.g. Movshon et al., 1978; Tolhurst & Dean, 1987; Albrecht & Geisler, 1991; Heeger, 1992*b*; DeAngelis et al., 1993; Anzai et al., 1999*b*). An expansive function such as half-squaring (Heeger, 1992*b*), when applied to broadly tuned input, will sharpen the output tuning of the cell by accentuating the difference between large and small inputs to the cell. For each cell, we estimated the magnitude of the exponent needed to match the predicted orientation-tuning curve with the measured tuning curve. The exponent is given by the ratio of the variances of the Gaussian fits to the two orientation-tuning curves.

A population distribution of the exponents is shown in Fig. 3a. To accurately predict the orientation-tuning curve a wide range of exponents from 0.57 to 14.96 (geometric mean 3.15) is required. For cells with an exponent near 1, the linear mechanism is sufficient to explain the sharpness of the orientation tuning. Therefore, the elongated pattern of feedforward LGN inputs could potentially account for the orientation selectivity of these cells. However, a majority of cells exhibit an exponent much greater than 1, which indicates that the linear mechanism, and certainly the elongated pattern of feedforward LGN inputs, is not enough to explain the sharpness of orientation tuning. In other words, cortical mechanisms play a significant role in sharpening the orientation tuning for these cells.

The distribution shown in Fig. 3a is somewhat broader than that reported in Anzai et al. (1999*b*); it contains several higher values. However, this could be due to the fact that effective contrast of the

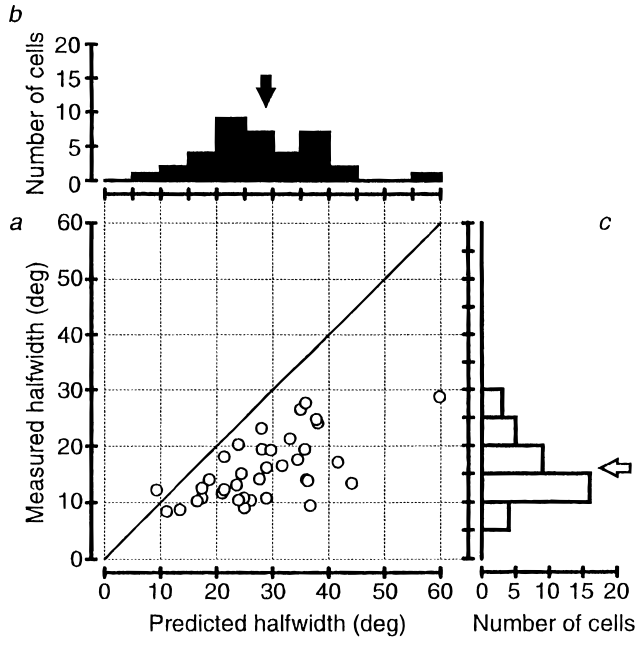

Fig. 2. (a) Scatter plot of the orientation-tuning halfwidths measured with sinusoidal gratings *versus* halfwidths as predicted from spatio-temporal RF profiles for the population of cells analyzed. Diagonal line indicates a one-to-one correspondence between measured and predicted tuning halfwidths. The majority of points fall below the line, indicating that the measured halfwidth tends to be smaller than predicted. (b) Population distribution of halfwidths of predicted orientation tuning. The arrow indicates the mean of the distribution (mean = 28.3, s.d. = 10.0 deg). (c) Population distribution of halfwidths of measured orientation tuning. The arrow indicates the mean of the distribution (mean = 15.8, s.d. = 5.7).

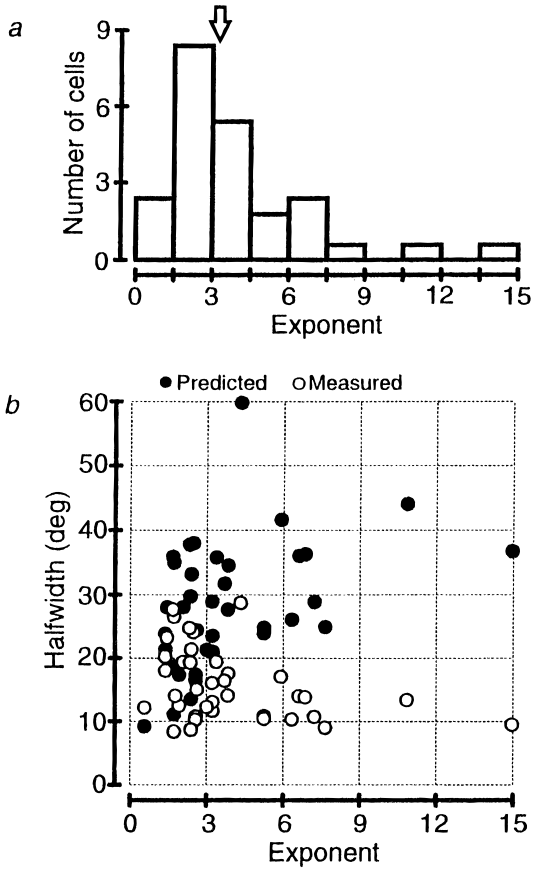

Fig. 3. (a) Distribution of exponents needed to match the measured and predicted orientation-tuning curves. The arrow indicates the geometric mean (3.15) of the distribution. (b) Relationship of exponent with halfwidth of measured and predicted orientation tuning. Filled circles correspond to predicted halfwidths and open circles correspond to measured halfwidths. There is a significant but weak positive correlation ($r^2 = 0.170$, slope = 1.434, $P < 0.05$) between exponents and halfwidths for the predicted curves, and a significant but weak negative correlation for the measured curves ($r^2 = 0.139$, slope = -0.732, $P < 0.05$).

grating stimulus is higher than that of the 2D m-sequence noise stimulus, and hence, the response gain of the neuron may have been different for each stimulus. This could bias exponents toward higher values. In fact, the distribution of exponents estimated from neuron's responses to stimuli of various contrasts, a condition that may be more analogous to the one in our study, exhibits a shape similar to the distribution in Fig. 3a (Albrecht & Hamilton, 1982).

Because an expansive nonlinearity has the effect of sharpening tuning, we would expect that the higher the exponent the sharper the orientation tuning. Fig. 3b shows the relationship between the magnitude of the exponent and the halfwidth of tuning. The halfwidths of the measured (open circles) and predicted (filled circles) orientation-tuning curves are plotted as a function of the exponent for each cell. There is a weak but significant positive correlation of exponents with predicted tuning halfwidth ($r^2 = 0.170$, slope = 1.434, $P < 0.05$), and a weak but significant negative correlation of exponents with measured tuning halfwidths ($r^2 = 0.139$, slope = -0.732, $P < 0.05$). This indicates that there is a tendency for cells whose RF properties impose only broad orientation selectivity to have a large exponent which makes their output very sharply tuned for orientation.

The results shown in Fig. 3 suggest that the cortical nonlinearity plays a significant role in sharpening the orientation tuning for some cells. However, as shown in Fig. 2, the linear mechanism alone can provide a moderate to narrow orientation tuning. By definition, the narrowness of the predicted tuning width is solely attributed to the RF geometry such as the size and shape. Next, we describe how the predicted tuning width depends on the RF geometry and examine if the measured tuning width also exhibits a similar dependency.

As illustrated in Fig. 1b, the predicted orientation-tuning curve is obtained as a section along the semicircle that goes through the RF in the frequency domain. Therefore, moving the RF in the frequency domain away from the origin and decreasing the extent along the v axis both serve to decrease the orientation-tuning halfwidth. In other words, the orientation-tuning halfwidth is proportional to the standard deviation (σ_v) along the v dimension of the RF in the frequency domain, and is inversely proportional to the optimal spatial frequency (f_o) of the cell. Since σ_v and f_o are inversely proportional to the subregion length (s_L) and width (s_W), respectively [see eqns. (4) and (5)],

$$\text{Orientation-tuning halfwidth} \propto s_W/s_L = 1/AR, \tag{7}$$

where *AR* denotes the subregion aspect ratio as defined in eqn. (3). Intuitively, the more elongated the subregions are, the narrower the orientation tuning becomes. When the relationship of eqn. (7) is plotted on a log–log axis, it becomes a straight line with a slope of -1.

Fig. 4a shows the predicted (filled circles) and measured (open circles) tuning halfwidth as a function of the subregion aspect ratio on a log–log axis. As expected, the predicted orientation-tuning halfwidth is inversely proportional to the subregion aspect ratio. The slope of the regression line is -0.854 ($r^2 = 0.832$, $P < 0.01$, log–log axis). However, the measured orientation-tuning halfwidths scatter uniformly within the triangular region bounded by the predicted halfwidths and the constant lower limit (about 8 deg) of the tuning halfwidth. We find only a weak correlation between the measured halfwidths and subregion aspect ratio, accounting for only 26% of the variance (Fig. 4a, $r^2 = 0.261$, slope = -0.431, $P < 0.01$, log–log axis). In other words, the RF shape as described by the subregion aspect ratio plays a minimal role in determining the measured tuning halfwidth. Watkins and Berkley (1974) also found a similar degree of correlation between the measured halfwidth and the subregion aspect ratio.

Having examined the dependency of orientation-tuning halfwidth on an RF shape parameter, we now examine the role of RF

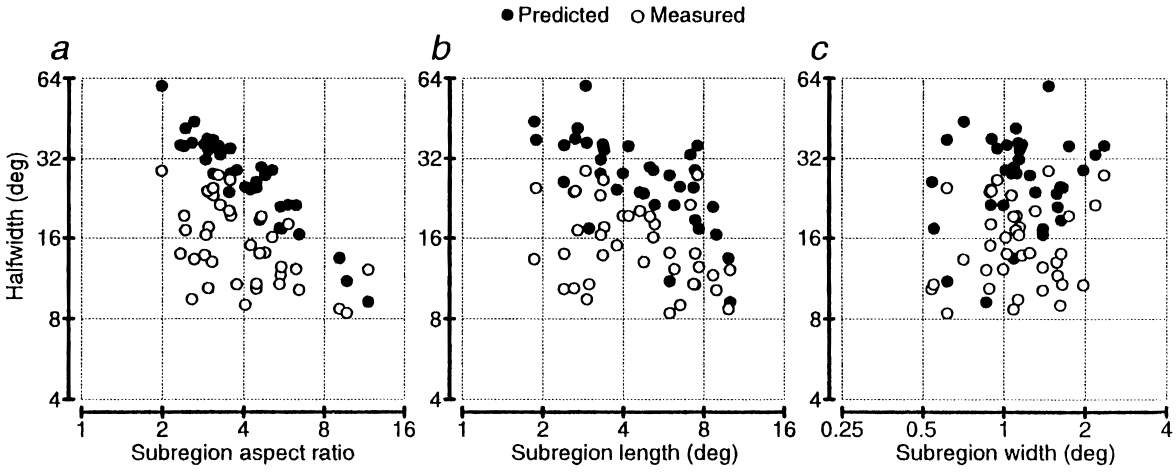

Fig. 4. (a) Relationship of subregion aspect ratio with halfwidths of measured and predicted orientation tuning. Filled circles correspond to predicted halfwidths and open circles correspond to measured halfwidths. Subregion aspect ratio accounts for 83% of the variance ($r^2 = 0.832$, slope = -0.854, $P < 0.01$, log–log axis) in predicted tuning halfwidth but only 26% of the variance ($r^2 = 0.261$, slope = -0.431, $P < 0.01$, log–log axis) in measured tuning. (b) Relationship of subregion length with halfwidths of measured and predicted orientation tuning. Symbols are the same as part (a). Subregion length is correlated with predicted halfwidths ($r^2 = 0.413$, slope = -0.514, $P < 0.01$, log–log axis), but not with measured halfwidth ($r^2 = 0.099$, slope = -0.227, $P = 0.058$, log–log axis). (c) Relationship of subregion width with halfwidths of measured and predicted orientation tuning. Symbols are the same as part (a). Subregion width is not correlated with predicted halfwidths ($r^2 = 0.034$, slope = 0.196, $P = 0.277$, log–log axis) or measured halfwidths ($r^2 = 0.027$, slope = 0.158, $P = 0.334$, log–log axis).

size parameters. As indicated by eqn. (7), the predicted orientation-tuning halfwidth depends on two RF size parameters; subregion length and width. Figs. 4b and 4c show orientation-tuning halfwidths as a function of subregion length and width, respectively. The predicted halfwidth tends to decrease with subregion length (Fig. 4b, $r^2 = 0.413$, slope $= -0.514$, $P < 0.01$, log–log axis). This is consistent with the prediction from eqn. (7). However, the predicted tuning halfwidth shows no significant correlation with the subregion width (Fig. 4c, $r^2 = 0.034$, slope $= 0.196$, $P = 0.277$, log–log axis). This is simply because the range of subregion width is quite small (0.54–2.35 deg) compared to that of subregion length (1.86–10.02 deg) and subregion width and length are not strongly correlated ($r^2 = 0.307$, slope $= 0.415$, $P < 0.01$, log–log axis). On the other hand, the measured tuning halfwidths show no significant correlation with either subregion length (Fig. 4b, $r^2 = 0.099$, slope $= -0.227$, $P = 0.058$, log–log axis) or subregion width (Fig. 4c, $r^2 = 0.027$, slope $= 0.158$, $P = 0.334$, log–log axis), thus indicating that orientation-tuning halfwidth is independent of the RF size. Watkins and Berkley (1974) found orientation-tuning halfwidth to increase with the RF size. However, this could be partially due to the fact that complex cells, which are known to exhibit somewhat larger RF size (Hubel & Wiesel, 1962) and broader orientation tuning (Henry et al., 1974; Ikeda & Wright, 1975) than simple cells, are included in their data with simple cells.

Finally, we have examined the halfwidth of orientation tuning as a function of the number of subregions in the RF. With more subregions, a grating of nonoptimal orientation might overlap more subregions and thus be a poor stimulus for the cell. We found that this is not the case; there is no significant correlation between number of subregions and measured orientation-tuning halfwidth ($r^2 = 0.031$, slope $= 0.287$, $P = 0.299$).

Discussion

We find that measured orientation tuning of simple cells in the cat's striate cortex deviates from the orientation tuning predicted by linear spatial summation in two fundamental ways. First, the measured tuning curves are more sharply tuned than the predicted curves (Fig. 2). Second, the measured tuning halfwidths are largely independent of RF shape and size, the factors that determine the halfwidth of the predicted tuning (Fig. 4).

Both of these differences between measured and predicted orientation tuning can be accounted for by the effects of a cortical nonlinearity in the form of an expansive exponent. We calculated the magnitude of the exponent needed to be applied to predicted orientation tuning to match the measured orientation tuning (Fig. 3a). Cells whose RF characteristics impose only broad orientation tuning tend to have large exponents that ensure that their output becomes highly selective for orientation (Fig. 3b). Our overall conclusion is that both linear and nonlinear mechanisms play a role in the sharpness of orientation tuning. However, since the nonlinear mechanism can change the tuning halfwidth by 2–3-fold and serves to make tuning halfwidth independent of RF parameters, it therefore plays quite an important role in determining the sharpness of orientation tuning.

RF shape, in particular the aspect ratio of subregions, has been an area of intense interest because feedforward models suggest that simple cells acquire orientation selectivity from elongated patterns of LGN inputs (for a review, see Sompolinsky & Shapley, 1997). Aspect ratio of subregions has been measured quantitatively in both extracellular and intracellular recordings. Our distribution of subregion aspect ratios is consistent with other extracellular measurements (Jones & Palmer, 1987*a*) but has a larger mean (4.3 *vs.* 1.7) than aspect ratios measured intracellularly (Pei et al., 1994). Intracellular recordings measure aspect ratios based on excitatory postsynaptic potentials (EPSPs) and are thought to faithfully reflect the excitatory input from LGN neurons. Therefore, the intracellular data suggest that elongated patterns of LGN inputs alone are not sufficient to account for the sharpness of orientation tuning (see also Volgushev et al., 1996). Our results indicate that cortical factors such as spatially opponent inhibition (Ferster, 1988; Troyer et al., 1998), which is reflected in extracellular recordings, increase the subregion aspect ratio, but not enough to account for the measured orientation-tuning width.

Our finding that the linear mechanism is generally insufficient to account for the sharpness of measured orientation tuning indicates that a nonlinear process of cortical origin plays a significant role. The linear mechanism has two origins: subcortical and cortical. Cross-correlation analysis of LGN and simple cells have shown that LGN input helps to determine the linear filtering properties (Reid & Alonso, 1995), but cortical mechanisms such as a spatially opponent inhibition (Ferster, 1988) are also thought to contribute to the linear filtering properties (Pollen & Ronner, 1982; Troyer et al., 1998). Our data therefore do not discriminate between the contribution of feedforward LGN input and that of the cortical network in determining optimal orientation preference. However, they do show that the nonlinearity, which we attribute to an expansive exponent, accounts for the sharpness of orientation tuning. Because spatial summation of synaptic inputs to simple cells is remarkably linear (e.g. Jagadeesh et al., 1997) and the effects of subcortical nonlinearites do not seem to appear in cortical neurons (e.g. Emerson et al., 1989), the expansive nonlinearity must be attributed to cortical factors. In other words, nonlinear cortical mechanisms serve to sharpen orientation tuning.

Potential neural mechanisms that could give rise to an expansive nonlinearity run the gamut from intracellular to network properties (for a review, see Koch & Poggio, 1992). For example, nonlinear interactions in the dendritic arbor and the spike-triggering mechanism at the soma of simple cells might work to produce spiking with an exponential relationship to the synaptic input. On the other hand, cortical network properties might give rise to an expansive nonlinearity as well. Contrast normalization of the type proposed by Heeger (Heeger, 1992*a*) could dynamically adjust the response gain of a neuron and mimic an expansive nonlinearity when the effects are averaged over time (Heeger, 1992*b*). There is also a suggestion that recurrent cortical excitation could amplify input signals (e.g. Douglas et al., 1995) and could therefore provide the neuronal basis for the expansive nonlinearity. Such recurrent excitation has been used to explain the sharpness of orientation and directional selectivities (Douglas et al., 1995; Somers et al., 1995).

The ability of the cortical nonlinearity to shape orientation tuning has important implications for the properties of simple cells. A perfectly linear simple cell would have to rely on RF attributes such as subregion aspect ratio and size to determine the sharpness of orientation tuning. On the other hand, an expansive nonlinearity can act to determine the sharpness of tuning independent of these parameters. This serves to ensure that orientation is represented equally well regardless of RF size and shape.

Acknowledgments

This work was supported by research and CORE grants from the National Eye Institute (EY01175 and EY03176). J.L. Gardner was supported by an NSF graduate fellowship.

References

Albrecht, D.G. & Geisler, W.S. (1991). Motion selectivity and the contrast–response function of simple cells in the visual cortex. *Visual Neuroscience* **7**, 531–546.

Albrecht, D.G. & Hamilton, D.B. (1982). Striate cortex of monkey and cat: Contrast response function. *Journal of Neurophysiology* **48**, 217–237.

Anzai, A., Ohzawa, I. & Freeman, R.D. (1999*a*). Neural mechanisms for encoding binocular disparity: Receptive field position *versus* phase. *Journal of Neurophysiology* **82**, 874–890.

Anzai, A., Ohzawa, I. & Freeman, R.D. (1999*b*). Neural mechanisms for processing binocular information. I. Simple cells. *Journal of Neurophysiology* **82**, 891–908.

Campbell, F.W., Cleland, B.G., Cooper, G.F. & Enroth-Cugell, C. (1968). The angular selectivity of visual cortical cells to moving gratings. *Journal of Physiology* (London) **198**, 237–250.

Chapman, B., Zahs, K.R. & Stryker, M.P. (1991). Relation of cortical cell orientation selectivity to alignment of receptive fields of the geniculocortical afferents that arborize within a single orientation column in ferret visual cortex. *Journal of Neuroscience* **11**, 1347–1358.

DeAngelis, G.C., Ohzawa, I. & Freeman, R.D. (1993). Spatiotemporal organization of simple-cell receptive fields in the cat's striate cortex: II. Linearity of temporal and spatial summation. *Journal of Neurophysiology* **69**, 1118–1135.

DeAngelis, G.C., Robson, J.G., Ohzawa, I. & Freeman, R.D. (1992). Organization of suppression in receptive fields of neurons in cat visual cortex. *Journal of Neurophysiology* **68**, 144–163.

Douglas, R.J., Martin, K.A.C. & Whitteridge, D. (1991). An intracellular analysis of the visual responses of neurones in cat visual cortex. *Journal of Physiology* **440**, 659–696.

Douglas, R.J., Koch, C., Mahowald, M., Martin, K.A.C. & Suarez, H.H. (1995). Recurrent excitation in neocortical circuits. *Science* **269**, 981–985.

Emerson, R.C., Korenberg, M.J. & Citron, M.C. (1989). Identification of intensive nonlinearities in cascade models of visual cortex and its relation to cell classification, In *Advanced Methods of Physiological System Modeling, Vol. 2,* ed. Marmarelis, V., pp. 97–111. New York: Plenum.

Ferster, D. (1986). Orientation selectivity of synaptic potentials in neurons of cat primary visual cortex. *Journal of Neuroscience* **6**, 1284–1301.

Ferster, D. (1988). Spatially opponent excitation and inhibition in simple cells of cat visual cortex. *Journal of Neuroscience* **8**, 1172–1180.

Ferster, D., Chung, S. & Wheat, H. (1996). Orientation selectivity of thalamic input to simple cells of cat visual cortex. *Nature* **380**, 249–252.

Hata, Y., Tsumoto, T., Sato, H., Hagihara, K. & Tamura, H. (1988). Inhibition contributes to orientation selectivity in visual cortex of cat. *Nature* **335**, 815–817.

Heeger, D.J. (1992*a*). Normalization of cell responses in cat striate cortex. *Visual Neuroscience* **9**, 181–197.

Heeger, D.J. (1992*b*). Half-squaring in responses of cat striate cells. *Visual Neuroscience* **9**, 427–443.

Henry, G.H., Dreher, B. & Bishop, P.O. (1974). Orientation specificity of cells in cat striate cortex. *Journal of Neurophysiology* **37**, 1394–1409.

Hubel, D.H. & Wiesel, T.N. (1959). Receptive fields of single neurones in the cat's striate cortex. *Journal of Physiology* **148**, 574–591.

Hubel, D.H. & Wiesel, T.N. (1961). Integrative action in the cat's lateral geniculate body. *Journal of Physiology* **155**, 385–398.

Hubel, D.H. & Wiesel, T.N. (1962). Receptive fields, binocular interaction and functional architecture in the cat's visual cortex. *Journal of Physiology* **160**, 106–154.

Ikeda, H. & Wright, M.J. (1975). Retinotopic distribution, visual latency and orientation tuning of 'sustained' and 'transient' cortical neurones in area 17 of the cat. *Experimental Brain Research* **22**, 385–398.

Jagadeesh, B., Wheat, H.S., Kontsevich, L.L., Tyler, C.W. & Ferster, D. (1997). Direction selectivity of synaptic potentials in simple cells of the cat visual cortex. *Journal of Neurophysiology* **78**, 2772–2789.

Jones, J.P. & Palmer, L.A. (1987*a*). The two-dimensional spatial structure of simple receptive fields in cat striate cortex. *Journal of Neurophysiology* **58**, 1187–1211.

Jones, J.P. & Palmer, L.A. (1987*b*). An evaluation of the two-dimensional Gabor filter model of simple receptive fields in cat striate cortex. *Journal of Neurophysiology* **58**, 1233–1258.

Koch, C. & Poggio, T. (1992). Multiplying with synapses and neurons. In *Single Neuron Computation,* ed. McKenna, T., Davis, J. & Zornetzer, S.F., pp. 315–345. San Diego, California: Academic Press.

Levick, W.R. (1972). Another tungsten microelectrode. *Medical and Biological Engineering* **10**, 510–515.

Movshon, J., Thompson, I. & Tolhurst, D. (1978). Spatial summation in the receptive fields of simple cells in the cat's striate cortex. *Journal of Physiology* (London) **283**, 53–77.

Nelson, S., Toth, L., Sheth, B. & Sur, M. (1994). Orientation selectivity of cortical neurons during intracellular blockade of inhibition. *Science* **265**, 774–777.

Pei, X., Vidyasager, T.R., Volgushev, M. & Creutzfeldt, O.D. (1994). Receptive-field analysis and orientation selectivity of postsynaptic potentials of simple cells in cat visual cortex. *Journal of Neuroscience* **14**, 7130–7140.

Pollen, D.A. & Ronner, S.F. (1982). Spatial computation performed by simple and complex cells in the visual cortex of the cat. *Vision Research* **22**, 101–118.

Press, W.H., Flannery, B.P., Tevkolsky, S.A. & Vetterling, W.T. (1988). Numerical recipes in C: The art of scientific computing. Cambridge: Cambridge University Press.

Reid, R.C. & Alonso, J.-M. (1995). Specificity of monosynaptic connections from thalamus to visual cortex. *Nature* **378**, 281–284.

Rose, D. & Blakemore, C. (1974). An analysis of orientation selectivity in the cat's visual cortex. *Experimental Brain Research* **20**, 1–17.

Sillito, A.M. (1975). The contribution of inhibitory mechanisms to the receptive field properties of neurones in the striate cortex of the cat. *Journal of Physiology* (London) **250**, 305–329.

Sillito, A.M., Kemp, J.A., Milson, J.A. & Berardi, N. (1980). A re-evaluation of the mechanisms underlying simple cell orientation selectivity. *Brain Research* **194**, 517–520.

Skottun, B.C., De Valois, R.L., Grosof, D.H., Movshon, J.A., Albrecht, D.G. & Bonds, A.B. (1991). Classifying simple and complex cells on the basis of response modulation. *Vision Research* **31**, 1079–1086.

Somers, D.C., Nelson, S.B. & Sur, M. (1995). An emergent model of orientation selectivity in cat visual cortical simple cells. *Journal of Neuroscience* **15**, 5448–5465.

Sompolinsky, H. & Shapley, R. (1997). New perspectives on the mechanisms for orientation selectivity. *Current Opinion in Neurobiology* **7**, 514–522.

Sutter, E.E. (1992). A deterministic approach to nonlinear systems analysis. In *Nonlinear Vision: Determination of Neural Receptive Fields, Function, and Networks,* ed. Pinter, R.B. & Nabet, B., pp. 171–220. Boca Raton, Florida: CRC Press.

Tolhurst, D.J. & Dean, A.F. (1987). Spatial summation by simple cells in the striate cortex of the cat. *Experimental Brain Research* **66**, 607–620.

Troyer, T.W., Krukowski, A.E., Priebe, N.J. & Miller, K.D. (1998). Contrast-invariant orientation tuning in cat visual cortex: Thalamocortical input tuning and correlation-based intracortical connectivity. *Journal of Neuroscience* **18**, 5908–5927.

Tsumoto, T., Eckart, W. & Creutzfeldt, O.D. (1979). Modification of orientation sensitivity of cat visual cortex neurons by removal of GABA-mediated inhibition. *Experimental Brain Research* **34**, 351–363.

Volgushev, M., Vidyasagar, T.R. & Pei, X. (1996). A linear model fails to predict orientation selectivity of cells in the cat visual cortex. *Journal of Physiology* **496**, 597–606.

Watkins, D.W. & Berkley, M.A. (1974). The orientation selectivity of single neurons in cat striate cortex. *Experimental Brain Research* **19**, 433–446.